



DE88015482

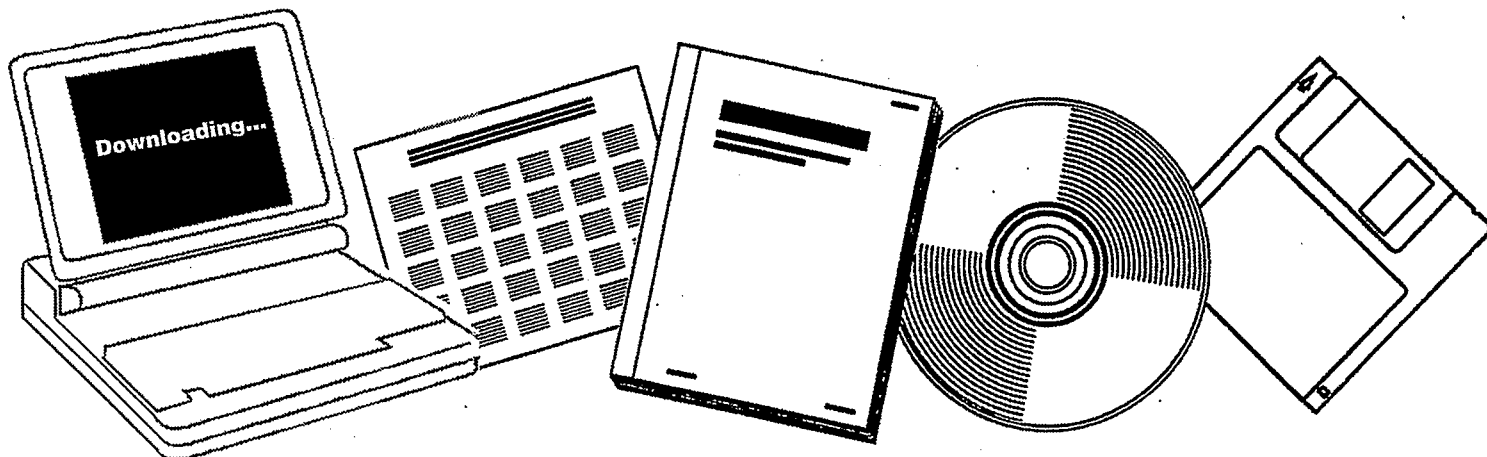
NTIS

One Source. One Search. One Solution.

HEAT TRANSFER INVESTIGATIONS IN A SLURRY BUBBLE COLUMN: QUARTERLY REPORT OF THE PERIOD APRIL--JUNE 1988

ILLINOIS UNIV. AT CHICAGO CIRCLE. DEPT.
OF CHEMICAL ENGINEERING

1988



U.S. Department of Commerce
National Technical Information Service

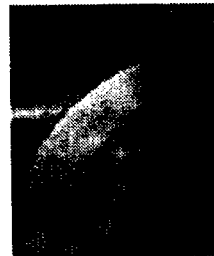
One Source. One Search. One Solution.

NTIS



Providing Permanent, Easy Access to U.S. Government Information

National Technical Information Service is the nation's largest repository and disseminator of government-initiated scientific, technical, engineering, and related business information. The NTIS collection includes almost 3,000,000 information products in a variety of formats: electronic download, online access, CD-ROM, magnetic tape, diskette, multimedia, microfiche and paper.



Search the NTIS Database from 1990 forward

NTIS has upgraded its bibliographic database system and has made all entries since 1990 searchable on www.ntis.gov. You now have access to information on more than 600,000 government research information products from this web site.

Link to Full Text Documents at Government Web Sites

Because many Government agencies have their most recent reports available on their own web site, we have added links directly to these reports. When available, you will see a link on the right side of the bibliographic screen.

Download Publications (1997 - Present)

NTIS can now provide the full text of reports as downloadable PDF files. This means that when an agency stops maintaining a report on the web, NTIS will offer a downloadable version. There is a nominal fee for each download for most publications.

For more information visit our website:

www.ntis.gov



U.S. DEPARTMENT OF COMMERCE
Technology Administration
National Technical Information Service
Springfield, VA 22161

DOE/PC/90008--T4

DE88 015482

HEAT TRANSFER INVESTIGATIONS IN A SLURRY BUBBLE COLUMN

Quarterly Report of the Period April-June 1988

S.C. Saxena, Principal Investigator
R. Vadivel, Research Associate
A.K. Verma, Research Associate

University of Illinois at Chicago
Department of Chemical Engineering
810 South Clinton, Chicago, IL 60607

DISCLAIMER

This report was prepared as an account of work sponsored by an agency of the United States Government. Neither the United States Government nor any agency thereof, nor any of their employees, makes any warranty, express or implied, or assumes any legal liability or responsibility for the accuracy, completeness, or usefulness of any information, apparatus, product, or process disclosed, or represents that its use would not infringe privately owned rights. Reference herein to any specific commercial product, process, or service by trade name, trademark, manufacturer, or otherwise does not necessarily constitute or imply its endorsement, recommendation, or favoring by the United States Government or any agency thereof. The views and opinions of authors expressed herein do not necessarily state or reflect those of the United States Government or any agency thereof.

Prepared for the United States Department of Energy, Pittsburgh Energy Technology
Center, Under DOE Contract DE-AC22-86 PC 90008
DOE Project Manager: Mr. George Cinquegrane

MASTER

OBJECTIVES

To investigate the heat transfer characteristics in two slurry bubble columns (Diameters 10.8 and 30.5 cm) as a function of system and operating parameters.

SUMMARY

Detailed measurements of gas holdup in the small 10.8 cm diameter column have been completed for the two-phase air-water system. Experiments have been conducted in the semi-batch mode as well as in the continuous mode as a function of air velocity. Experiments are done to see the influence, if any, of the 19 mm diameter axial probe in the column on air holdup. The experiments are also conducted for the three-phase, air-water-glass bead system, and phase holdup are measured as a function of air velocity, water column height, solids concentration, and with and without the presence of an axial heat transfer probe. The heat transfer coefficient between the single axial 19 mm diameter probe and the three-phase dispersion is measured as a function of time, air velocity and solids concentration. In order to understand the mechanism of heat transfer, the variation of local temperature history of an element of the heater surface is recorded for the two-and three-phase systems.

Two pressure profile measuring devices for the larger 30.5 cm diameter slurry bubble column have been completed and measurements of gas holdup as a function of air velocity, initial water column height, and with and without the presence of heat transfer probe are reported for the two-phase air-water system.

Interpretation of the gas holdup data both total and local is completed on the basis of available correlations. The heat transfer data are examined and analyzed on the basis of data of the other workers, correlations and theoretical models.

Three technical papers describing and discussing the results obtained in the earlier period of this contract as well as during the current reporting period have been completed and submitted to the journals for publication and presentation at the International Conferences.

DESCRIPTION OF TECHNICAL PROGRESS

TASKS 2 AND 3

- A. Gas holdup measurement in the air-water and air-water-glass beads systems**

To gain understanding of the nature of gas holdup in a liquid as the operating and system parameters are changed, a series of experiments is conducted with air-water system in a 10.8 cm internal diameter column. The pressure profile is measured by a set of liquid manometers along the column to yield the average value of the air holdup in the entire water column as well as of the local air holdup in different sections of the column along its height. The experiments are conducted both in the semi-batch mode (water flow velocity is zero) as well as in the continuous mode (water flow velocity has a finite value). The air velocity is varied in the range 3.2 to 33.2 cm/s and air holdup is measured for both increasing and decreasing air velocities. In the former, the air velocity is steadily increased to the desired value in steps and the height of the air-water dispersion is brought to a fixed value (170.12 cm) when the pressure readings are taken and then the air and water flows are instantly stopped and the settled height of the dispersion is noted again. These data enable to compute both the average and the local values of the air holdup. Similar data are taken in the decreasing velocity mode except here first the air velocity is increased in steps and brought to the maximum value, thereafter the air flow is decreased in steps and at each step the makeup water is added to bring the dispersion height to 170.12 cm. The water flow velocities (V) are arbitrarily chosen as 0, 3.8, 5.1, and 9.2 mm/s. The air holdup values are measured for the water column with no internal as well as for the case when a cylindrical probe, 19 mm outer diameter, is placed along its axis. The data taken are displayed in Figures 1-3, and are discussed in the following. The uncertainty associated with the determination of average air holdup is about 2% while that associated with the local air holdup is dependent on the air velocity as well as on the value of the air holdup. At the top end of the column, the air holdup is large due to foam formation and the pressure difference uncertainty is relatively large because of the small magnitude of the pressure difference. The uncertainty is estimated for the top section to be ± 5 percent at lowest air velocity and ± 50 percent at the highest air velocity. In the remaining sections of the column the uncertainties are ± 5 and ± 35 percent for the lowest and the highest air velocities.

In Figure 1 the average air holdup data exhibit negligible hysteresis effect as the values are approximately the same (within an average deviation of $\pm 5\%$) for increasing and decreasing air velocities. The dashed curves are drawn through the decreasing air flow velocity points on eye judgement. For zero liquid velocity data points are taken for both with and without the cylindrical probe internal. The two sets of data are in qualitative as well as generally in quantitative agreement with each other within the range of experimental error in the $\bar{\epsilon}_g$ values. This is not surprising as the internal-occupies only four percent of the column cross-section. The qualitative trend of the variation of $\bar{\epsilon}_g$ with U as seen in Figure 1 is superposition of the normal variation of $\bar{\epsilon}_g$ with U (i.e. monotonic increase of $\bar{\epsilon}_g$

with increasing U) and that which is produced due the formation and break up of foam structure as the gas velocity is increased.

The effect of liquid flow rate on gas holdup in the present air flow velocity range is found to be small. The average of the four sets of values differ on the average by a maximum amount of about 8 percent from the individual values. The data of Figure 1 are also compared with the predictions based on the correlations of Hughmark¹ and Hills² which were examined on the basis of other experimental data in the progress report for the month of March 1988. The lack of agreement between the computed and experimental values is due to the foam formation. It appears that probably Hughmark correlation is a reasonable choice for calculating the holdup with liquid flow in the absence of foam formation.

In Figure 2 the qualitative variations of local air holdup along the column height do not exhibit any pronounced or systematic differences for the increasing or decreasing air velocity for the entire air velocity range. Certain qualitative trends are evident and may be stated to infer the nature of bubble dynamics in the column. In the lower section of the column $H < 50$ cm, the bubble coalescence becomes increasingly pronounced as the air velocity is increased. This behavior causes the air holdup to decrease with increasing gas velocity in the column region $H < 50$ cm. For $50 < H < 100$ cm, the gas holdup remains constant almost over the entire air velocity range. For the column region $100 < H < 150$ cm, the gas holdup increases with H , the increase being pronounced for higher gas velocities. This is attributed to the formation of foam in the column. It is also clear from these plots that the formation and breakup of foam takes place in the major portion of the column, $H > 50$ cm, and more so for higher gas velocities. The average air holdup values are also shown in this Figure by dashed horizontal lines and these highlight the departure in the values of the local air holdup from the average air holdup values.

Figure 3 represents data similar to that of Figure 2 except that the column has an axial 19 mm diameter cylindrical probe occupying only about four percent of the column cross-section. The general variation of air holdup data is similar to that of Figure 2 and it is also somewhat expected in view of the small cross-section of the probe relative to column cross section.

On the small column, measurements of gas holdup have been conducted using glass beads in the size range 75-125 μm . The sieve analysis results giving the particle size distribution and computation of mean particle diameter are reported in Table 1. Other relevant properties of these solids are also listed in this table.

The procedure of making a run with three-phase systems for holdup measurements is as follows. The column was filled with distilled water upto a stagnant or slumped height, H_L , of 90 cm. Next a known amount of solids was

added to the column, and the column height of the slurry, H_{SL} , was noted. The computed values of slurry concentrations, C_s , defined as the ratio of the mass of solids to the volume of slurry are reported in Table 2. Also shown in this table are the mass fraction of solids in the slurry, m_f , defined as the ratio of the mass of solids to the mass of slurry. The air at a known flow rate was bubbled through the column and the expanded height of the slurry, H_T , was noted when the steady state was reached (about fifteen minutes). The average values of gas, solid and liquid holdup were determined from the following relations:

$$\epsilon_g = (H_T - H_{SL}) / H_T \quad (1)$$

$$\epsilon_s = (H_{SL} - H_L) / H_T = (1 - \epsilon_g) (H_{SL} - H_L) / H_{SL} \quad (2)$$

$$\epsilon_L = (H_L / H_T) = 1 - \epsilon_g - \epsilon_s \quad (3)$$

These holdup were measured for decreasing values of the air velocity with the heat transfer probe present in the column. In other words, the air velocity was increased to its maximum value and H_T was recorded and thereafter the air velocity was decreased continuously in steps and corresponding H_T values were noted. Computed values of ϵ_g , ϵ_s and ϵ_L as a function of air velocity and for five values of C_s including zero are shown in Figure 4. Some qualitative trends are obvious in this plot and are reported below.

The average air holdup, ϵ_g , decreases as the slurry concentration, C_s , is increased (curves 3-5) in relation to values corresponding to $C_s = 0$ (curve 1). This decreasing air holdup is due to increased coalescence of bubbles. The solids holdup, ϵ_s , increases with increase in C_s at a given U , and for a given C_s it is found to slowly decrease with increasing U . In general, ϵ_L seems to decrease with increasing U and increases with increasing C_s . Curve 2 referring to the lowest C_s value represents a somewhat different variation for ϵ_g and ϵ_L . It is attributed to be due to the foam formation which disappears at higher C_s values, based on visual observations.

The installation of the pressure measuring circuit in the larger 0.305 m diameter column is completed. This comprises of two independent parallel circuits. In one circuit the pressure drop across the column and across three sections along its height is measured by liquid manometers while the flow from the column to the measuring circuit is prevented by the application of appropriate purge air pressure with the help of suitably designed flow systems. In the other circuit these column

pressure drops are sensed by a pressure transducer and read on a calibrated digital monitor. The initial testing of the system is successfully completed and the measurement of air holdup taken to-date are discussed in the following.

In the larger 30.5 cm internal diameter glass column, measurements have been completed for the average ($\bar{\epsilon}_g$) and local (ϵ_g) air holdup as a function of air velocity in the range 1.6 to 37.6 cm/s at ambient temperature (298 K). Tap water was filled up-to the initial slumped height of 140 cm, and the column was aerated upto the maximum air velocity. The expanded column height was recorded and thereafter the air velocity was reduced in steps and the air-water dispersion height was noted. From these records the air holdup was computed as a function of air velocity. Some foaming was observed particularly at the top of the dispersion and it was relatively much less than what was observed earlier in the smaller column. Similar data were taken with distilled water. Both these sets of data points are shown in Figure 5, and these are in good agreement with each other.

Another experiment was conducted for the initial unaerated distilled water column height of 95 cm and these results are also shown in Figure 5. It is important to note that the air holdup values are consistently larger than the values corresponding to the initial water column height of 140 cm. This would suggest that bubble coalescence played a role so that the bubble diameter and hence the air holdup is dependent upon the height of the dispersion. The greater the height, the smaller is the holdup.

Also shown in Figure 5 are the values obtained in the smaller 10.8 cm diameter column for the same initial water column height of 95 cm and other conditions which are with the larger column. It will be seen that the agreement in the values of air holdup for the two columns is good at lower and higher air velocities. The difference in the middle air velocity range is due to increased foaming in the smaller column. Based on these results, it would appear that the bubbling phenomenon and the hydrodynamics of these two column is quite similar as long as no foaming occurs.

Also reported in this figure are the values of the average air holdup as obtained on the two columns with the heat transfer probe present. The two sets of values are in fair agreement with each other and varying values of H_g in the two cases can lead to some differences also. Computed values of air holdup due to Hughmark¹ and Hills are also shown in this figure. The former seems to represent our measurements better than the latter.

The larger column has pressure measuring probes installed along its height at distances of 4, 52.3, 160.5 and 218.9 cm above the air distributor plate. The

measurements of pressure drops were taken for the above mentioned two initial heights of the water column. From these data, the air holdup values for these column sections were computed and these values of the local air holdup are shown in Figure 6. Curve a refers to the initial water column height of 95 cm, and represents the air holdup values (local) in the column section enclosed between 4 and 52.3 cm above the distributor plate. The average air holdup values for the entire column as shown in Figure 5 are also displayed in Figure 6 as curve a'. These values are consistently greater than the local values. This will clearly suggest that the local air holdup values are increasing with height in the column.

Curves b and c of Figure 6 refer to the initial distilled water column height of 140 cm and for the dispersion sections enclosed between column heights of 4 and 52.3 cm, and 52.3 and 160.5 cm respectively. Curve C represents slightly higher air holdup values, than curve b. The average holdup values (b' and c') shown in Figure 6 are greater than the values of curves b and c for the same air velocity. curves b' and c' are identical in magnitude. This conclusively suggests that there is a small increase in the air holdup values with increase in height in the column. Increasing bubble coalescence with height in the column as suggested by the results of Figure 5 cannot explain this qualitative dependence of local air holdup on column height and it is attributed to increased foaming in the column which increases in magnitude with increase in column height. This last qualitative statement concerning foaming is in conformity with the visual observations in both the columns though in the smaller column only this fact is abundantly clear.

B. Heat transfer measurements in the air-water and air-water-glass beads systems

Heat transfer coefficient between the 19 mm probe with the heater in the middle section and the slurry is measured at various U . In each case, the gas velocity was increased to a high value so that the solids are well dispersed and thereafter its value was adjusted to the desired value. For gas velocities smaller than 10.3 cm/s, the heater surface was not completely covered by the three-phase dispersion. The measurements were taken as a function of time and the computed heat transfer coefficient values are shown in Figure 7 for the lowest and highest C_s values. As emphasized earlier, the suspension temperature rises with time, the rise being more at lower gas velocities. The steady state values are plotted in Figure 8 for all the C_s values. For $C_s = 0$, h_w increases with U and becomes constant after $U = 25$ cm/s, curve a.

As increasing amounts of solids are added, h_w variation for $U < 20$ cm/s depends to some extent on C_s and appears to be constant for U values in the range

10 to 20 cm/s for specific values of C_s , curves b to e. The solids for these air velocities though suspended in water are not uniformly distributed in the column. The heater location in the column will play a role. The region $U > 25$ cm/s is more interesting and here it seems that h_w is constant over the range 25-35 cm/s and the value of C_s does not influence the value of h_w . However, h_w values for this three-phase system is only about 5% greater than the corresponding two-phase system values. This will suggest that the three-phase dispersion properties influence h_w in a complicated fashion.

With a view to understand the mechanism of heat transfer, the local temperature history of the heat transfer probe surface element is recorded in two- and three-phase dispersions. These results are displayed in Figures 9 and 10 respectively. It is clear from Figure 9 that the local surface temperature does not exhibit wide temperature fluctuations, suggesting thereby that the nature of the phase in contact with it does not significantly change. In particular, the surface never sees the pure discontinuous phase and the small temperature fluctuations may be due to the different mix of pure phases (air and water) in the dispersion element visiting the heater surface. A similar heat transfer process seems to be operative when glass beads are added to the dispersion, Figure 10. This qualitative picture of heat transfer also explains the observed results that h_w is fairly constant at higher gas velocities for two- and three-phase systems.

TASK 4

Analysis and interpretation of experimental data

In the January 1988 monthly report, we presented the heat transfer data for a 19 mm heat transfer probe immersed axially in the 10.8 cm diameter column and referring to air-water system in the semi-batch mode at 315 K as a function of air velocity. In the following these data are compared with the data available in the literature and then examined on the basis of various proposed correlations and heat transfer models. Our data are shown in Figure 11 and refer to the gas velocity range of 0.034 to 0.353 m/s and heat transfer coefficient, h_w , is represented in kW/m²K. These must be multiplied by 176.11 to get values in Btu/ hr ft²°F. The uncertainty of our h_w values is about ± 4.5 percent. It may be noted that we used a perforated plate distributor with 91 holes of 0.8 mm diameter in equilateral triangular pitch and having a fine wire mesh screen on the downstream side.

The data of Kolbel et al.³ taken in columns of diameter 19.2 and 29.2 fitted with a porous plate distributor are shown by curve b in Figure 11. In the

overlapping air velocity range their h_w values are in good agreement with our measured values. Fair et al.⁴ have used two columns of diameters 45.7 cm and 106.7 cm fitted with air sparger rings and measured h_w for the column wall and the air-water dispersion in the former, and for a fortytwo 3.8 cm diameter tube bundle for the latter. These data are in agreement with Kolbel et al.³ and with our data in the overlapping air velocity range. Burkerl⁵ data referring to h_w for an immersed heater surface are systematically smaller than the other measured values except at the lowest air velocity which is in agreement with that of Kolbel et al.³ data.

Hart⁶ reported h_w values for the column wall of 9.9 cm diameter equipped with a single nozzle (0.635 cm hole diameter) in the low air velocity range. These values are consistently greater than all the other reported values. Steff and Weinspach⁷ employed a 19 cm diameter column with a sintered plate distributor and measured h_w for the heated column walls. Their data in the higher velocity range are in agreement with our values but are greater than those of other workers and are smaller than that of Hart⁶ in the low velocity range. Hikita et al.⁸ have measured h_w for column walls of diameters 0.1 and 0.19 m both equipped with single nozzle air spargers in the high velocity range. Their data are systematically greater than all the other measured values. Kast⁹ have reported column wall (0.288 m diameter) to air-water dispersion heat transfer coefficient in the low velocity range. Their data are in disagreement with the three other sets of data available for the same gas range velocities. Their values are greater than those of Kolbel et al.³ but are smaller than those of Hart⁶, and Steff and Weinspach⁷.

From the above brief reference of seven sets of available data, it is clear that large scatter exists in the h_w values for air velocities below 2.0 cm/s. This velocity range is of relatively little importance, and sufficiently good agreement exists in the velocity range 2.0 to 36 cm/s except the data due to Burkel⁵ and Hikita et al.⁸ appear to be systematically lower and higher respectively. Our measured values are in good agreement with those of Steff and Weinspach⁷, Fair et al.⁴ and Kolbel et al.³. It is, therefore, concluded that our data are reliable and precise. The experimental technique employed and procedures adopted in the analysis of experimental data to compute h_w are unique and inspire confidence in the generated values. A more detailed examination of these experimental data is in progress.

In the progress report for the month of February 1988, we computed the error in the measured h_w values due to the errors in the operating and geometric parameters. It came out to be about 4.5%. The error due to the heat loss at the two ends was not accounted in this calculation. Its estimate is given in the following.

The general design of our heater section was given in the progress report for the month of November 1987. To estimate the loss of heat from the two ends of the heated brass section about 33.4 cm long, Delrin connector sections about 5 cm long, were used at the either ends. Two thermocouples in each of these insulating sections are installed at a separation distance of 3 cm. The knowledge of this temperature gradient in conjunction with the thermal conductivity of Delrin enables the calculation of the longitudinal leakage of thermal energy from the total energy supplied to the heater. In our calculation we have assumed a value of 1.7 W/mK (0.1 Btu/hr ft°F) for the thermal conductivity, a value typical for many thermal insulating materials such as ebonite, plastic celluloid etc. This suggests a correction of about 0.07% in the value of h_w . The thermal conductivity for Delrin is only 0.225 W/mK and the corresponding correction is only 0.0025%. The small magnitude of this correction justifies the simple method of calculation adopted here for h_w .

Fair et al.⁴ proposed the following correlation for h_w on the basis of their experimental data for gas velocities upto about 5 cm/s:

$$h_w = 8.850 U^{0.22} \quad (4)$$

The predicted values based on this correlation are shown in Figure 12 by curve a. It is seen that the calculated values are in reasonable agreement with the experimental values upto about 20 cm/s air velocity. As the gas velocity is increased the disagreement between the two sets of values increases and is about 13.5% at the highest gas velocity of 35 cm/s.

Hikita et al.⁸ developed the following correlation covering a wider range of air velocity (5.3 to 34 cm/s) and several liquids having widely different values for μ_L and σ :

$$\frac{h_w}{\rho_L C_{PL} U} \left(\frac{C_{PL} \mu_L}{k_L} \right)^{2/3} = 0.411 \left(\frac{U \mu_L}{\sigma} \right)^{-0.851} \left(\frac{\mu_L^4 g}{\rho_L \sigma^3} \right)^{0.308} \quad (5)$$

Prandtl number varied in the range 4.9 to 93, $(U \mu_L / \sigma)$ and $\mu_L^4 g / \rho_L \sigma^3$ in the ranges 0.00054 to 0.076 and 7.7×10^{-12} to 1.6×10^{-6} respectively. Predictions based on this correlation (curve b) are consistently greater than our present h_w values, the disagreement increasing with gas velocity and is about 57% at the highest gas

velocity. As discussed earlier, their data are much higher than all of the other data sets. As a further check of the validity of this correlation we fitted our data into the above relation and obtained the following equation:

$$\frac{h_w}{\rho_L C_{pL} U} \left(\frac{C_{pL} \mu_L}{k_L} \right)^2 = 0.271 \left(\frac{U \mu_L}{\sigma} \right)^{-0.851} \left(\frac{\mu_L g}{\rho_L \sigma^3} \right)^{0.308} \quad (6)$$

Computed values from equation (6) are shown as curve b' in Figure 12. It should be noted that this relation, in general, does not have the ability to reproduce the qualitative trend of h_w to be constant at higher gas velocities.

Deckwer¹⁰ examined a number of correlations which expressed Stanton number as a function of the product of Reynolds number, Froude number and Prandtl number^x, where x varied between 1.94 to 2.5. Further, he considered following Kast⁹ that the radial component of fluid velocity produced by the axial movement of bubble is an important parameter for heat transfer coefficient, and the Higbie¹¹ surface renewal model mimics the heat transfer process. The mean contact time of an eddy, θ , was obtained by using Kolmogoroff's theory of isotropic turbulence. This suggested that

$$h \propto k_L^{0.5} \rho_L^{0.75} C_{pL}^{0.5} \mu_L^{-0.25} g^{-0.25} U^{0.25} \quad (7)$$

Finally, the relationship proposed in the nondimensional form on the basis of experimental data is

$$St = 0.1 \left(Re Fr Pr^2 \right)^{-0.25} \quad (8)$$

This relation is valid only upto 10 cm/s air velocity. Values based on this relation are shown as curve c in Figure 12. The reproduction of experimental data is adequate upto $U = 10$ cm/s but the computed values systematically diverge from the experimental values as the air velocity increases. The maximum disagreement is about 26 percent at the highest gas velocity. In view of the nature and magnitude of the disagreement, it is inferred that the extrapolation of the above correlation at higher gas velocities is not valid. Joshi et al.¹² attributed this deficiency of the theory on the assumption that all the gas energy is dissipated in the liquid to create turbulence.

Joshi and Sharma¹³ have argued that the input gas energy is dissipated and consumed in various ways and only less than 10 percent is used to create liquid motion in the bubbly flow regime. They derived the following relation for the average liquid circulation velocity in a bubble column based on a circulation cell model:

$$V_c = 1.31 \left[g D_c (U - \bar{\epsilon}_g V_{b\infty}) \right]^{1/3} \quad (9)$$

Joshi et al.¹² contend that the enhancement of heat transfer from an immersed surface in a bubble column is due to the liquid circulation and proposed the following two relations for h_w . Based on the correlation for mechanically agitated contactors they found

$$\frac{h_w D_c}{k_L} = 0.48 \left[\frac{D_c^{1.33} g^{0.33} (U - \bar{\epsilon}_g V_{b\infty})^{1/3} \rho_L}{\mu_L} \right]^{0.66} \left(\frac{C_p \mu_L}{k_L} \right)^{1/3} \quad (10)$$

while pipe flow correlation leads to:

$$\frac{h_w D_c}{k_L} = 0.087 \left[\frac{D_c^{1.33} g^{1/3} (U - \bar{\epsilon}_g V_{b\infty})^{1/3} \rho_L}{\mu_L} \right]^{0.8} \left(\frac{C_p \mu_L}{k_L} \right)^{1/3} \quad (11)$$

Predictions based on the above two correlations are shown as curves d and e respectively in Figure 12. In these computations $V_{b\infty}$ is taken as 0.23 m/s following Joshi and Sharma¹⁴ which is based on Calderbank¹⁵ work for bubbles having diameters in the range 6 mm to 7.2 mm and U_G in the range 5 to 30 cm/s. $\bar{\epsilon}_g$ is estimated from

$$\bar{\epsilon}_g = U / (0.3 + 2U) \quad (12)$$

developed by Mashelkar¹⁶ for air water system. Both sets of computed values are systematically greater than the experimental values, the divergence is more pronounced for the curve d. At the highest gas velocity the difference in the calculated and experimental values are 47 and 30 percent for curves d and e

respectively. A more thorough and detailed assessment of the details of this model is in order and will be undertaken with the availability of more detailed experimental data in the future as our experimental work progresses.

Zehner^{17,18} has proposed a model based on the concept that a thermal boundary layer exists at the wall which is thinned at the places where bubbles are present. The length of the boundary layer is same as the distance between successive bubbles and is given by

$$\ell = d_b \left(\pi/6 \bar{\epsilon}_g \right)^{1/3} \quad (13)$$

In the computation a constant value of 7 mm is assumed for ℓ . The heat transfer through this boundary layer is the same as that over a flat heated plate and hence

$$h_w = 0.18 (1 - \bar{\epsilon}_g) \left[k_L^2 \rho_L^2 C_{pL} V_c / \ell \mu_L \right]^{1/3} \quad (14)$$

where

$$V_c = \left[\frac{1}{25} \left(\frac{\rho_L - \rho_g}{\rho_L} \right) g D_c U \right]^{1/3} \quad (15)$$

and

$$\bar{\epsilon}_g = U / \left[0.25 \exp(5 \bar{\epsilon}_g) \right] \quad (16)$$

Zehner¹⁵ proposed to use the above relation only upto U about 10 cm/s and assumed h_w to be constant thereafter. Computed values based on the above relation are shown as curve f in Figure 12. The increase in h_w for U greater than 10 cm/s is gradual but experimental data are under-predicted the disagreement being 7.5 percent at the highest gas velocity.

REFERENCES

1. G.A. Hughmark, Holdup and Mass Transfer in Bubble Columns, Ind. Eng. Chem. Process. Des. Dev. **6**, 218-220, 1967.

2. J.H. Hills, The Operation of a Bubble Column at High Throughputs I. Gas Holdup Measurements, *Chem. Eng. J.* 12, 89-99, 1976.
3. H. Kolbel, W. Siemes, R. Maas and K. Muller, Wärmeübergang an Blasensäulen, *Chemie. Ing. Techn.* 30, 400-404, 1958.
4. J.R. Fair, A.J. Lambright and J.W. Andersen, Heat Transfer and Gas Holdup in a Sparged Contactor, *Ind. Eng. Chem. Process. Des. Dev.* 1, 33-36, 1962.
5. W. Burkel, Der Wärmeübergang an Heiz-und Kühlflächen in Begasten, *Chemie. Ing. Techn.* 44, 265-268, 1972.
6. W.F. Hart, Heat Transfer in Bubble-Agitated System. A General Correlation, *Ind. Eng. Chem. Process Des. Dev.* 15, 109-114, 1976.
7. A. Steiff and P.M. Weinspach, Heat Transfer in Stirred and Non-Stirred Gas-Liquid Contactors., *Ger. Chem. Eng.* 1, 150-161, 1978.
8. H. Hikita, S. Asai, H. Kikukawa, T. Zaïke and M. Ohue, Heat Transfer Coefficient in Bubble Columns. *Ind. Eng. Chem. Process. Des. Dev.* 20, 540-545, 1981.
9. W. Kast, Analyse Des. Wärmeübergangs in Blasensäulen, *Int. J. Heat Mass Transfer*, 5, 329-336, 1962.
10. W.D. Deckwer, On the Mechanism of Heat Transfer in Bubble Column Reactors, *Chem. Engg. Sci.* 35, 1341-1345, 1980.
11. Higbie, R., The Rate of Absorption of a Pure Gas into a Still Liquid During Short Periods of Exposure, *Trans. Am. Inst. Chem. Engrs.* 35, 365-389, 1935.
12. J.B. Joshi, M.M. Sharma, Y.T. Shah, C.P.P. Singh, M. Ally and G.E. Klinzing, Heat Transfer in Multiphase Contactors, *Chem. Eng. Commun.* 6, 257-271, 1980.
13. J.B. Joshi and M.M. Sharma, Liquid Phase Backmixing in Sparged Contactors, *Canadian J. Chem. Eng.*, 56, 116-119, 1978.
14. J.B. Joshi and M.M. Sharma, A Circulation Cell Model for Bubble Columns, *Trans. Instn. Chem. Engrs.* 57, 244-251, 1979.
15. P.H. Calderbank, *The Chem. Engr.* (No 212): CE 209, 1967.

16. R.A. Mashelakr, Bubble Columns, Br. Chem. Eng. 15, 1297-1304, 1976.
17. P. Zehner, Momentum, Mass and Heat Transfer in Bubble Columns. Part 2. Axial Blending and Heat Transfer., Int. Chem. Engng. 26, 29-35, 1986.
18. P. Zehner, Momentum, Mass and Heat Transfer in Bubble Columns. Part I. Flow Model of the Bubble Column and Liquid Velocities, Int. Chem. Engng. 26, 22-28, 1986.

Nomenclature:

C_{pL}	=	Heat Capacity of the liquid, Ws/kgK
D_c	=	Column diameter, m
d_b	=	Bubble diameter, m
Fr	=	Froude number.
g	=	Acceleration due to gravity, m/s ²
H	=	Axial position in the bubble column, m
h_w	=	Heat-transfer coefficient, W/m ² K
k_L	=	Thermal conductivity of the liquid, W/mK
ℓ	=	Mean distance between the bubbles, m
Pr	=	Prandtl number ($C_{pL}\mu_L/k_L$), -
Re	=	Reynold's number ($d_b U \rho_L / \mu_L$), -
St	=	Stanton number ($h_w d_b / k_L$), -
U	=	Superficial air velocity, m/s
V_c	=	Liquid velocity defined by either equation (6) or (12), m/s
$V_{b_{slip}}$	=	Slip velocity of a bubble, m/s
$\bar{\epsilon}_g$	=	Average air holdup, -
ρ_L	=	Density of the liquid, kg/m ³
ρ_g	=	Density of the gas, kg/m ³
μ_L	=	Viscosity of the liquid, kg/ms
σ	=	Surface tension of the liquid, N/m

Table 1. Size distribution of glass beads.

U. S.A. Sieve number	Sieve Size (μm)	Avg. size, dpi (μm)	Mass of Solids (g)	Mass fraction of solids, w_i (-)	w_i/dpi ($1/\mu\text{m}$)
100-120	-150+125	137.5	10.1135	0.2519	0.001832
120-140	-125+106	115.5	25.4538	0.6339	0.005488
140-170	-106+ 90	98.0	4.2978	0.1070	0.001092
170-230	-90+ 63	76.5	0.2851	0.0072	0.000090

$$\Sigma (w_i / \text{dpi}) = 0.008502$$

$$\text{Average particle diameter, } \bar{d}_p = \frac{1}{\Sigma (w_i / \text{dpi})} = 117.6 \mu\text{m}$$

Density of glass = 2500 kg/m³

Table 2. Concentrations of slurries.

Mass of Solids (kg) (-)	Volume of Slurry x 10³ (m³)	C_s (kg/m³)	m_f
0.000	8.256	000	0.0000
0.906	8.622	105	0.0989
1.784	8.989	198	0.1777
2.770	9.356	296	0.2512
3.818	9.723	393	0.3162

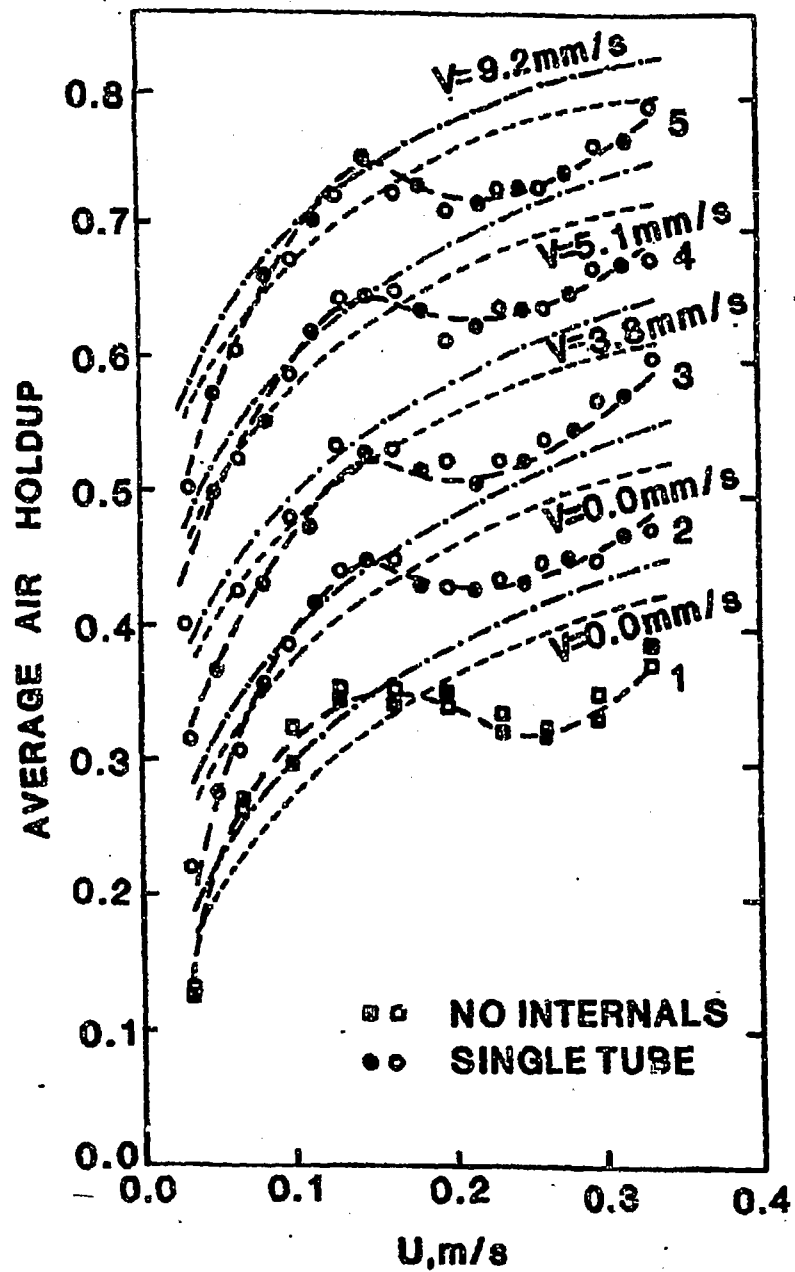


Figure 1. Average air holdup ($\bar{\epsilon}_g$) as a function of increasing and decreasing air velocity (U) in a water column with and without an axial cylindrical probe at different water flow velocities (V). Dashed and dot-dashed curves are due to Hughmark and Hills respectively.

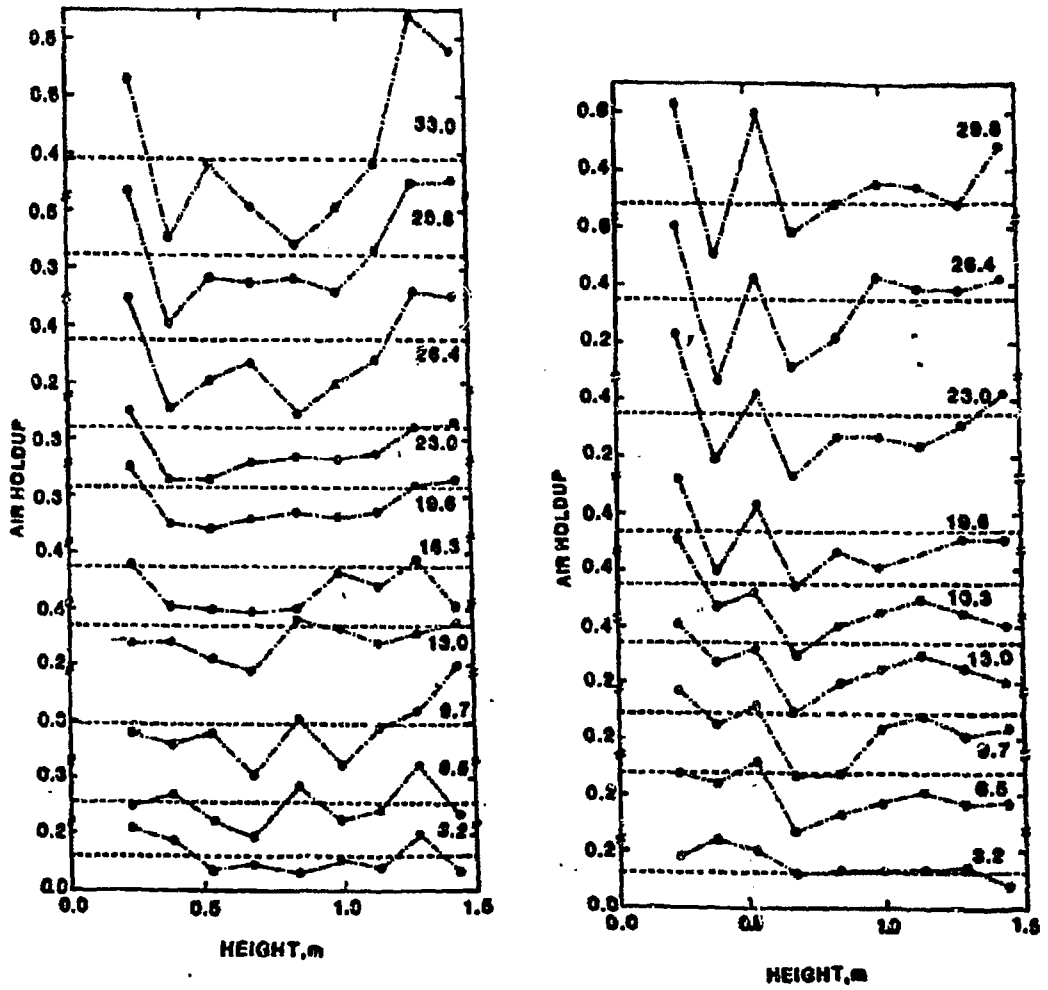


Figure 2. Variation of local air holdup along the water column at various increasing (A) and decreasing (B) air velocities, U (cm/s).

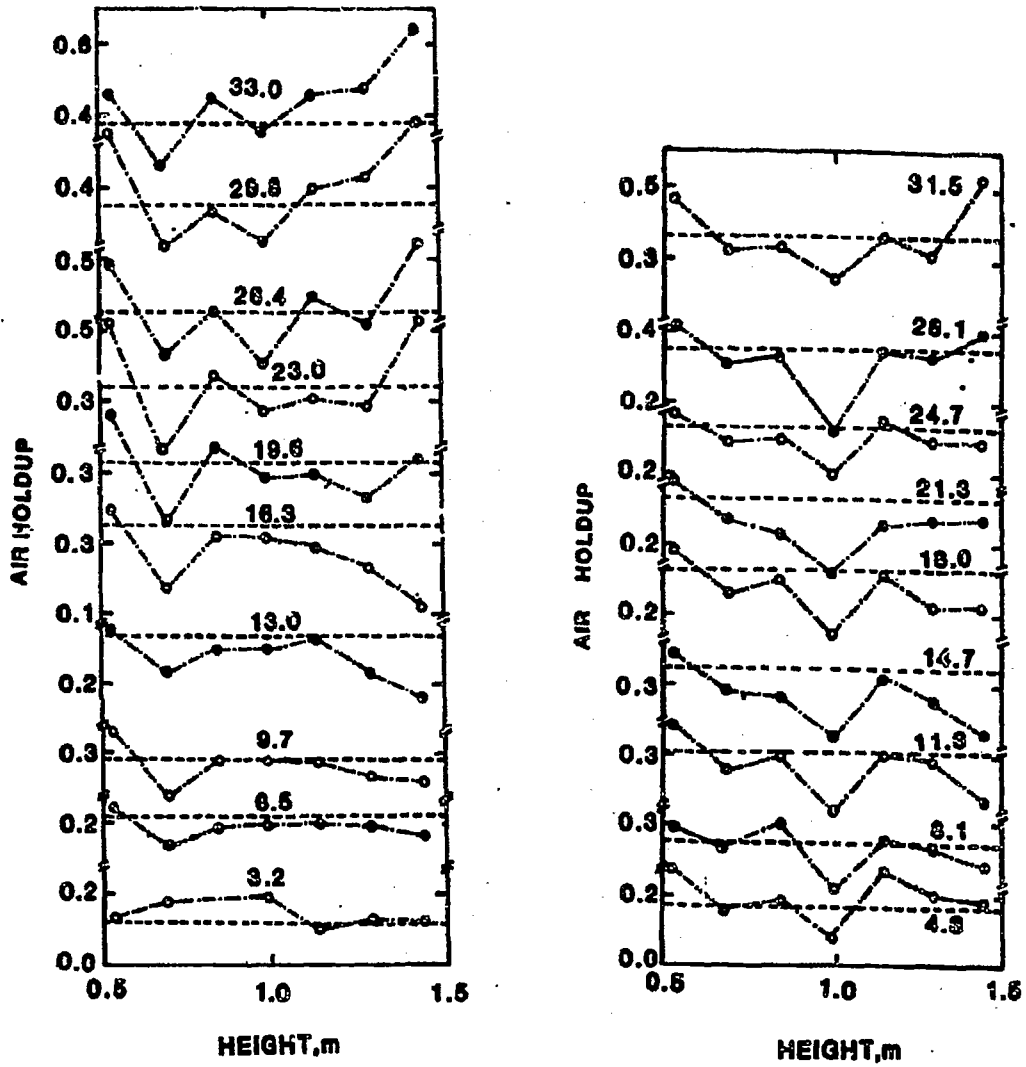


Figure 3. Variation of local air holdup along the water column with an axial cylindrical probe at various increasing (A) and decreasing (B) air velocities, U (cm/s).

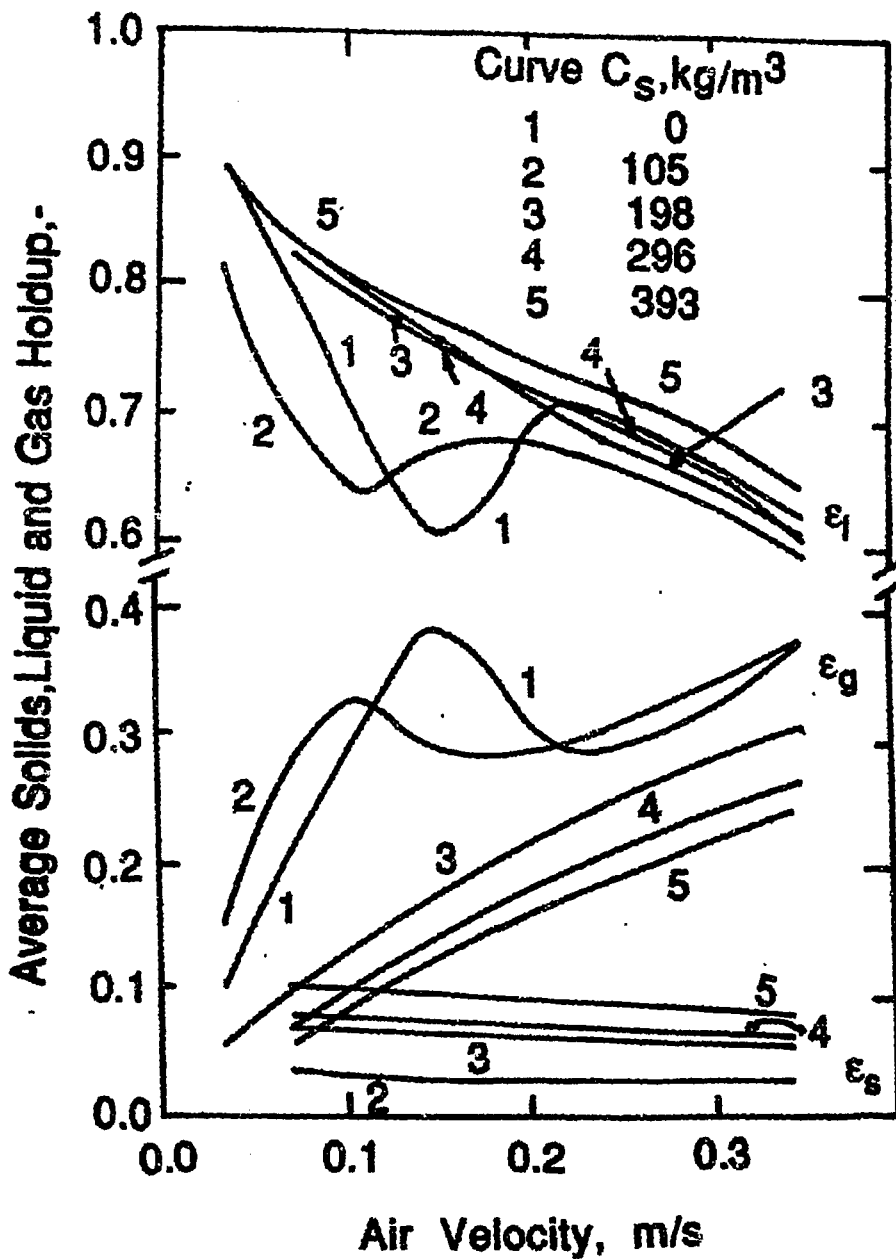


Figure 4. Variation of average solids, liquid and gas holdup as a function of decreasing air velocity for different solids concentrations in the column with a coaxial heat transfer probe at 294 K.

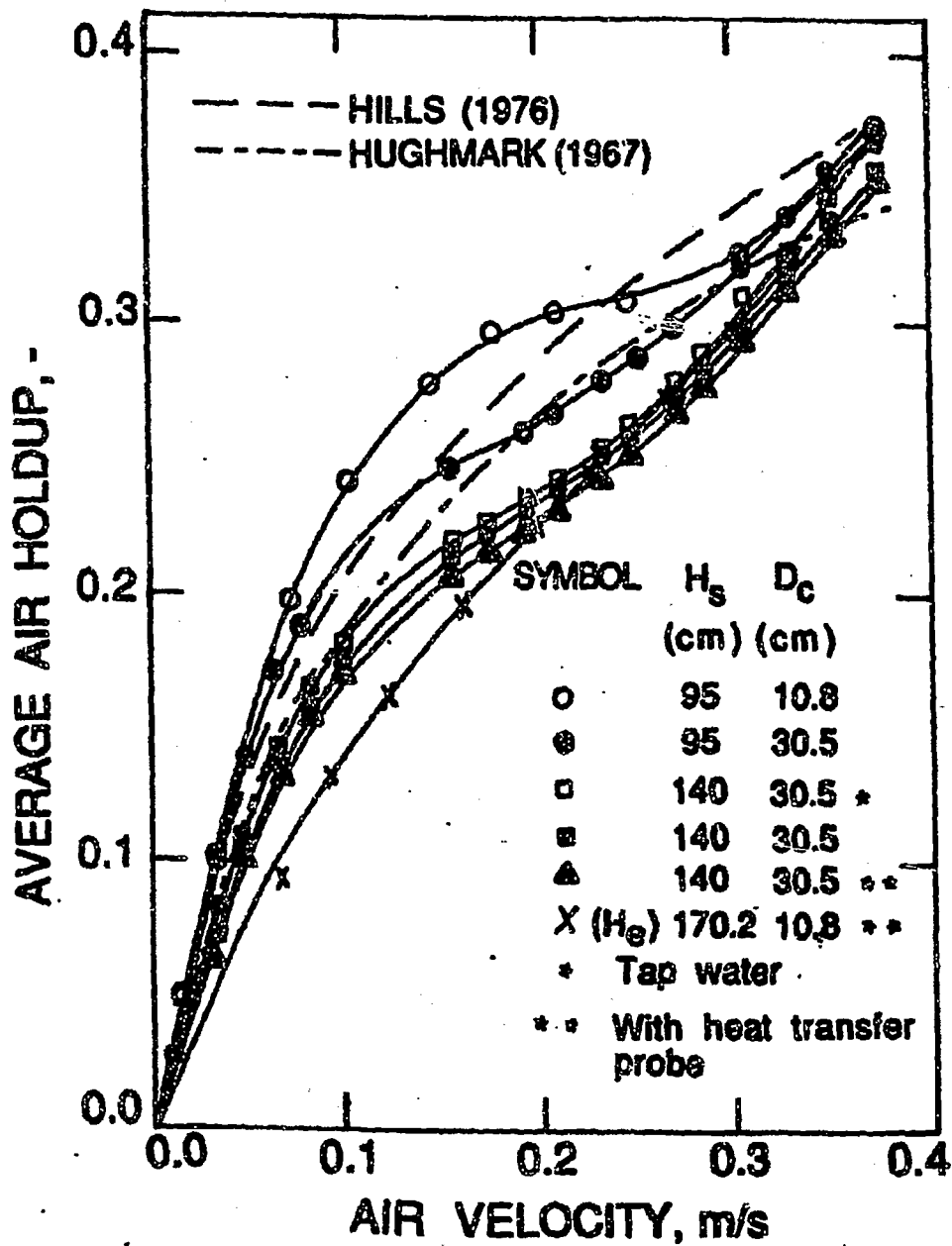


Figure 5. Variation of average air holdup with air velocity and initial water column height.

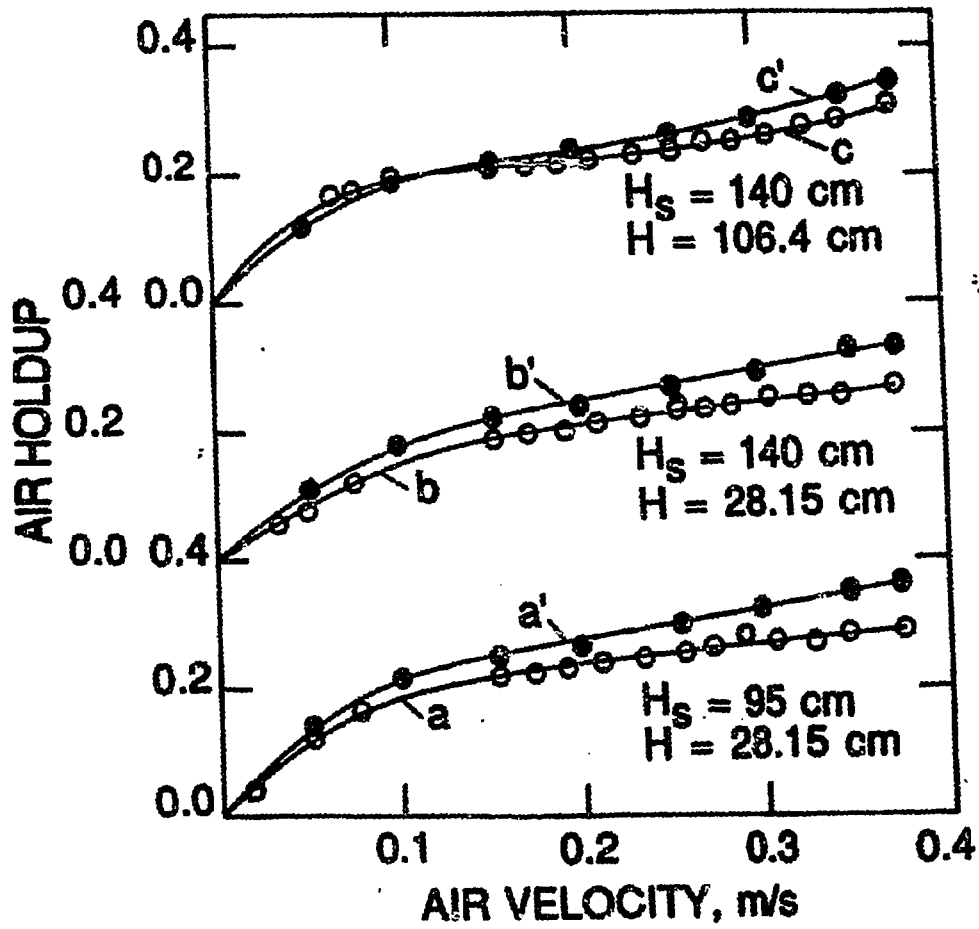


Figure 6. Variation of air holdup in different sections of the larger column with air velocity.

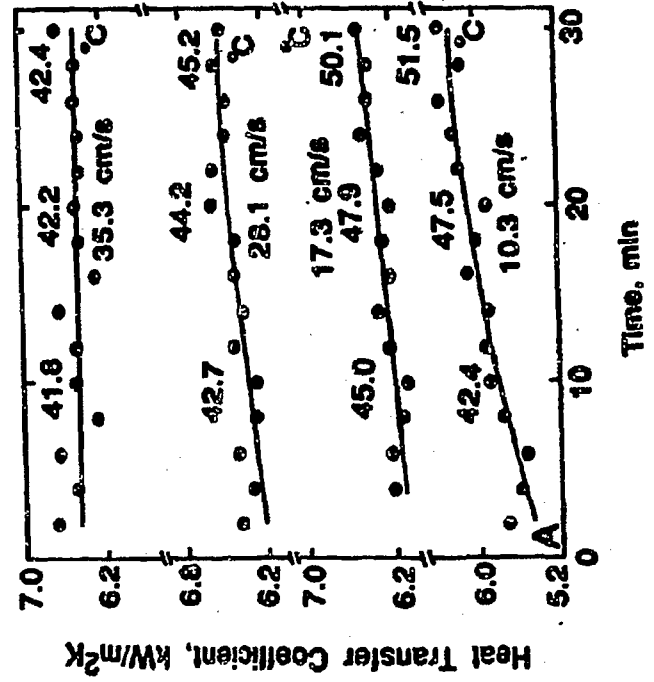
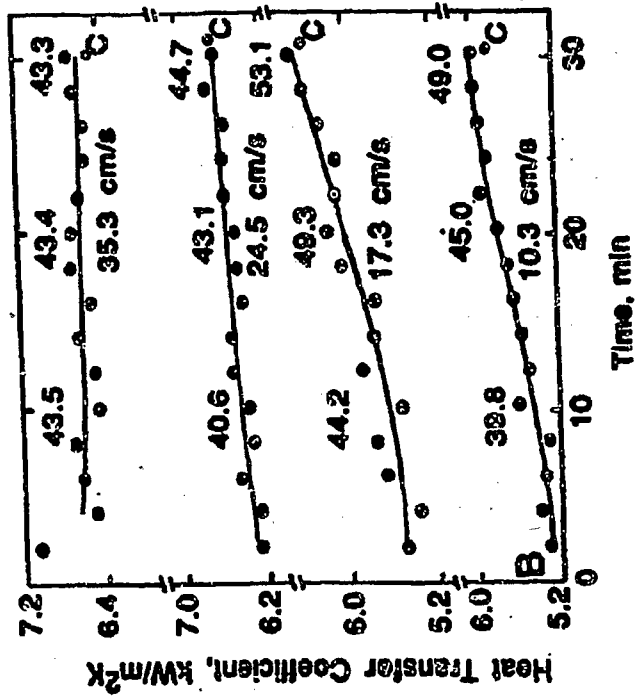


Figure 7. Variation of heat transfer coefficient with time at different air velocities for $C_s = 105 \text{ kg.m}^3$ (A) and $C_s = 393 \text{ kg.m}^3$ (B).

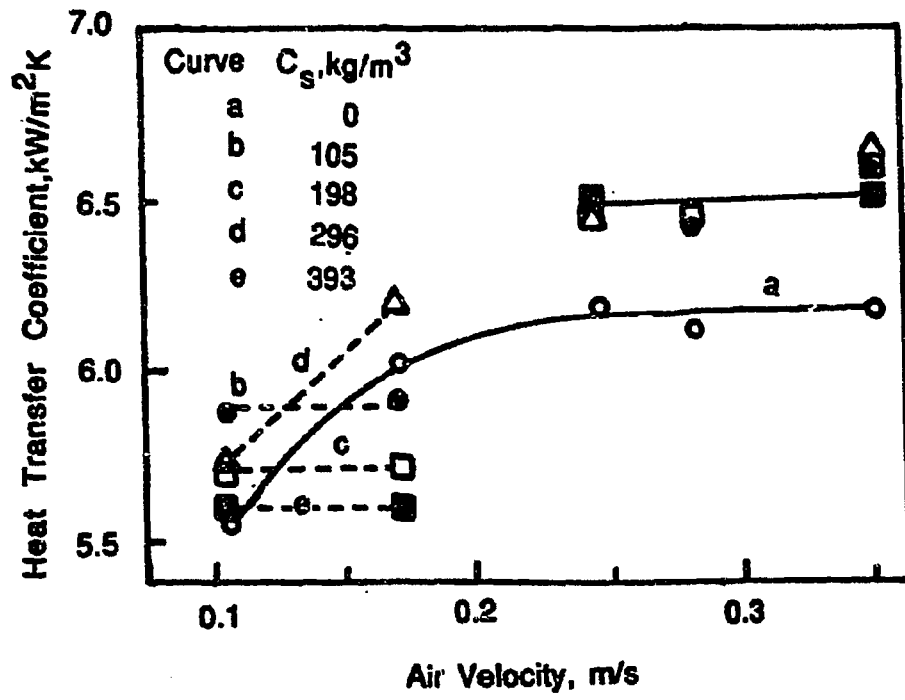


Figure 8. Variation of heat transfer coefficient with air velocity at different solids concentrations at 315 K.

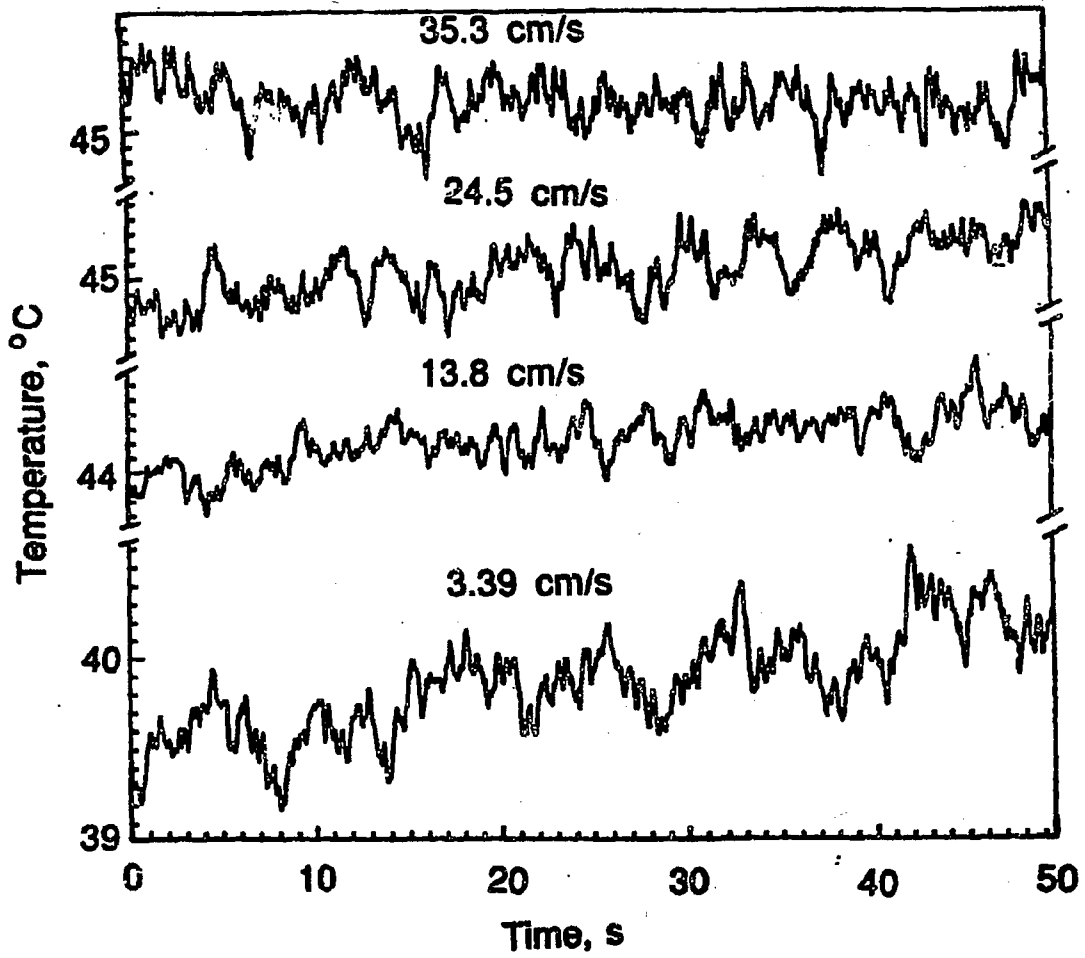


Figure 9. Variation of local temperature of heater surface with time at various air velocities for $C_s = 0 \text{ kg/m}^3$.

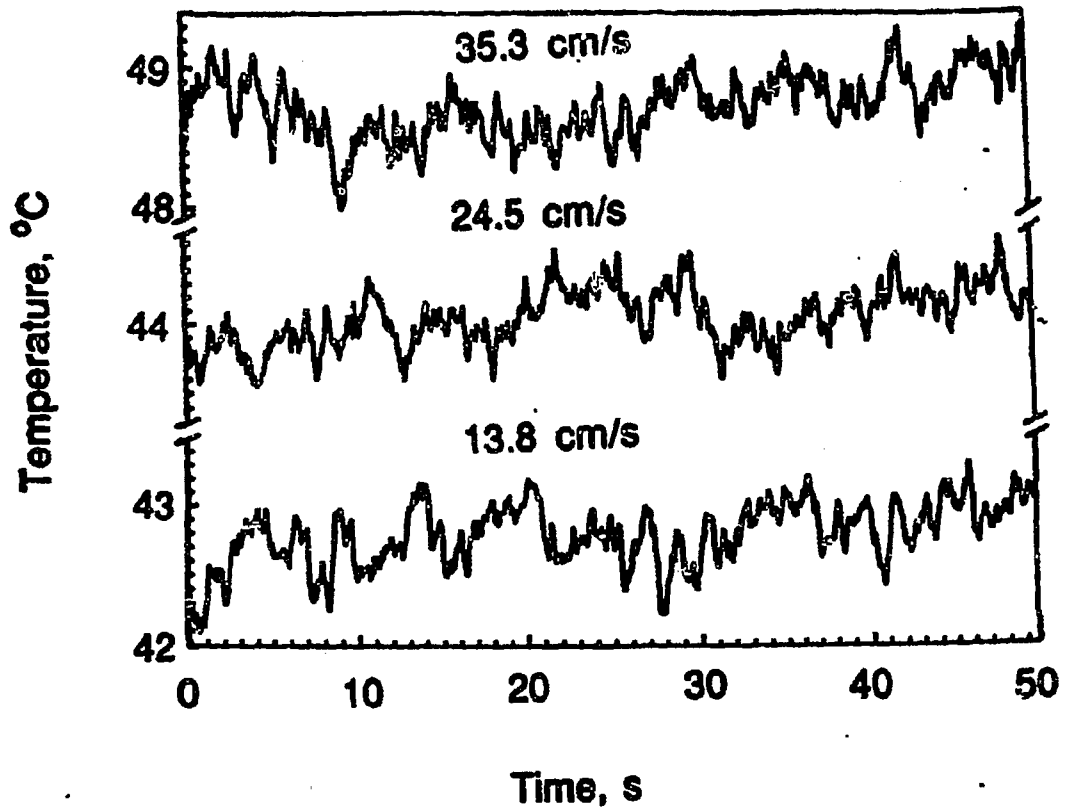


Figure 10. Variation of local temperature of heater surface with time at various air velocities for $C_s = 296 \text{ kg/m}^3$.

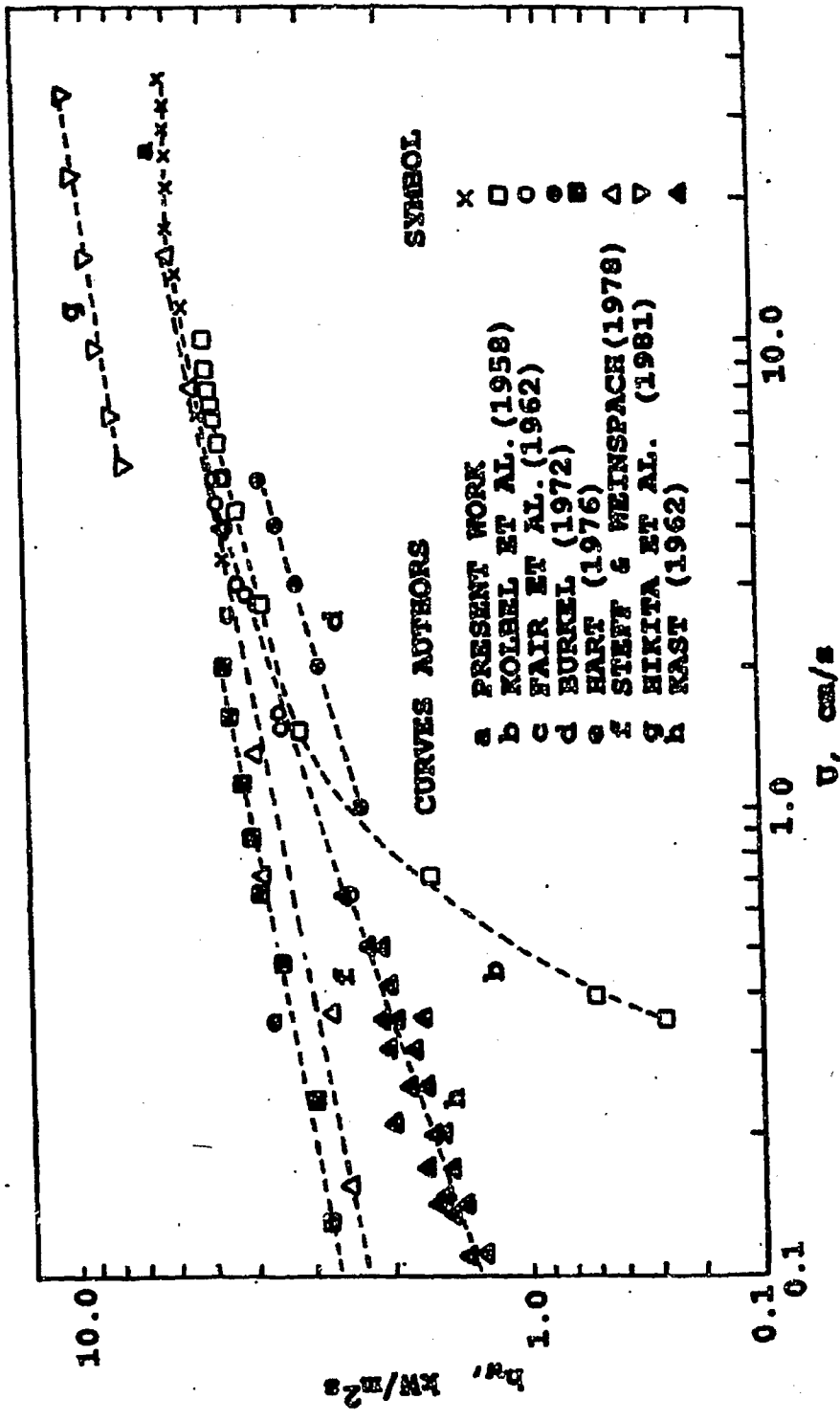


Figure 11. Comparison of the present experimental h_w values for air-water system with those of the other workers as a function of air velocity.

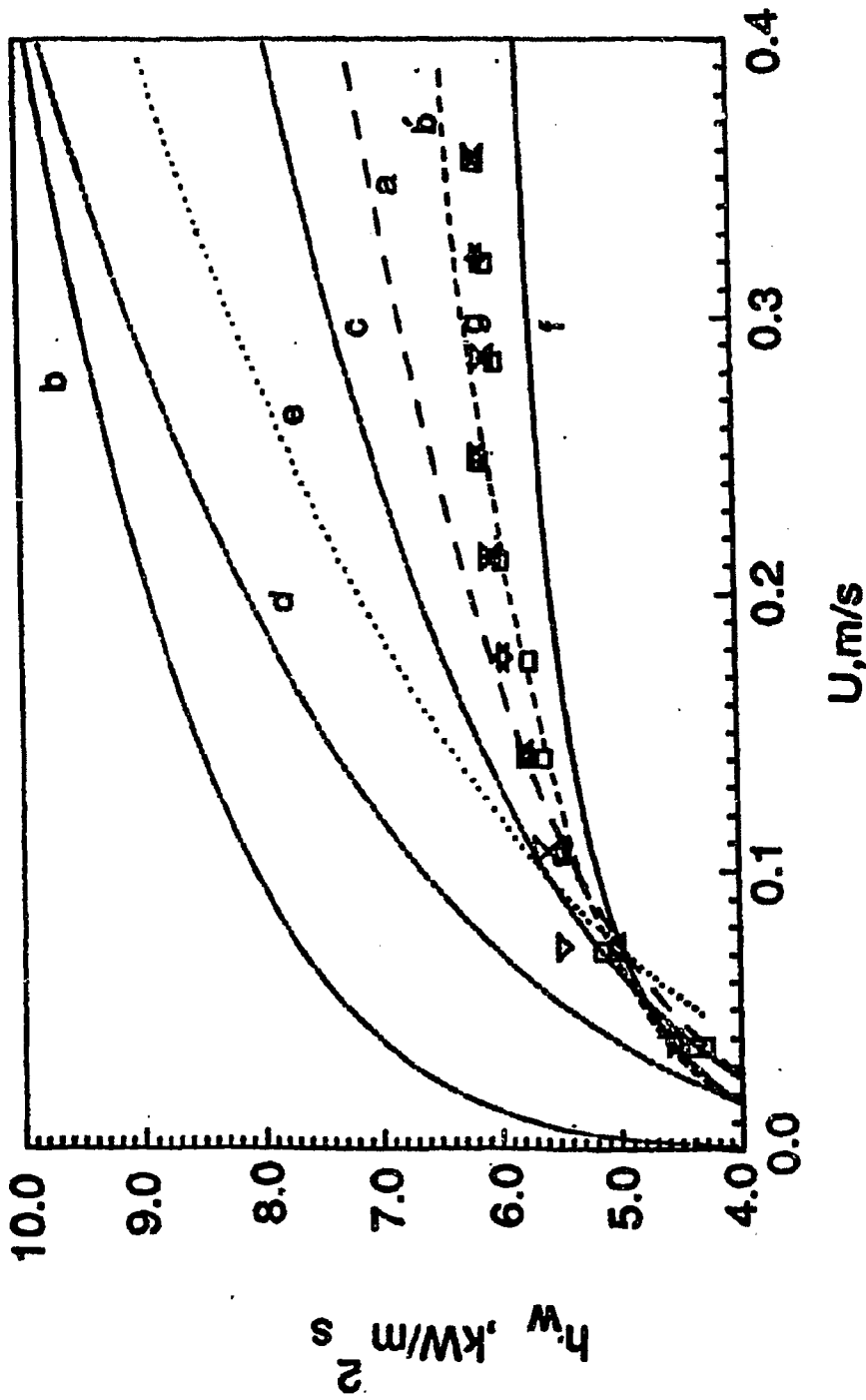


Figure 12. Comparison of the present experimental h_w values for air-water system with those predicted on the basis of different correlations and models as a function of air velocity. Curves a, c, (d and e) and f are due to Fair et al. (1962), Hikita et al. (1981), Deckwer (1980), Joshi et al. (1980), and Zehner (1986) respectively. Curve b' is according to a proposed correlation of equation (3)

SATISFACTION GUARANTEED

NTIS strives to provide quality products, reliable service, and fast delivery. Please contact us for a replacement within 30 days if the item you receive is defective or if we have made an error in filling your order.

▶ **E-mail: info@ntis.gov**

▶ **Phone: 1-888-584-8332 or (703)605-6050**

Reproduced by NTIS

National Technical Information Service
Springfield, VA 22161

This report was printed specifically for your order from nearly 3 million titles available in our collection.

For economy and efficiency, NTIS does not maintain stock of its vast collection of technical reports. Rather, most documents are custom reproduced for each order. Documents that are not in electronic format are reproduced from master archival copies and are the best possible reproductions available.

Occasionally, older master materials may reproduce portions of documents that are not fully legible. If you have questions concerning this document or any order you have placed with NTIS, please call our Customer Service Department at (703) 605-6050.

About NTIS

NTIS collects scientific, technical, engineering, and related business information – then organizes, maintains, and disseminates that information in a variety of formats – including electronic download, online access, CD-ROM, magnetic tape, diskette, multimedia, microfiche and paper.

The NTIS collection of nearly 3 million titles includes reports describing research conducted or sponsored by federal agencies and their contractors; statistical and business information; U.S. military publications; multimedia training products; computer software and electronic databases developed by federal agencies; and technical reports prepared by research organizations worldwide.

For more information about NTIS, visit our Web site at <http://www.ntis.gov>.

NTIS

**Ensuring Permanent, Easy Access to
U.S. Government Information Assets**



U.S. DEPARTMENT OF COMMERCE
Technology Administration
National Technical Information Service
Springfield, VA 22161 (703) 605-6000
